Surface temperature lapse rates over complex terrain: Lessons from the Cascade Mountains

Justin R. Minder,[1] Philip W. Mote,[2] and Jessica D. Lundquist[3]

[1]   The typically sparse distribution of weather stations in mountainous terrain inadequately resolves temperature variability. Accordingly, high-resolution gridding of climate data (for applications such as hydrological modeling) often relies on assumptions such as a constant surface temperature lapse rate (i.e., decrease of surface temperature with altitude) of 6.5°C km^{-1}. Using an example of the Cascade Mountains, we describe the temporal and spatial variability of the surface temperature lapse rate, combining data from: (1) COOP stations, (2) nearby radiosonde launches, (3) a temporary dense network of sensors, (4) forecasts from the MM5 regional model, and (5) PRISM geo-statistical analyses. On the windward side of the range, the various data sources reveal annual mean lapse rates of 3.9–5.2°C km^{-1}, substantially smaller than the often-assumed 6.5°C km^{-1}. The data sets show similar seasonal and diurnal variability, with lapse rates smallest (2.5–3.5°C km^{-1}) in late-summer minimum temperatures, and largest (6.5–7.5°C km^{-1}) in spring maximum temperatures. Geographic (windward versus lee side) differences in lapse rates are found to be substantial. Using a simple runoff model, we show the appreciable implications of these results for hydrological modeling.

1.   Introduction

[2]   Quantifying the distribution of temperature in complex terrain, especially the relationship between temperature and altitude, is essential for distinguishing where precipitation falls as rain or snow, for accurately modeling streamflow and ecosystem distributions, and for understanding decadal trends in snowpack and glacier volume. However, the sparsity of long term surface temperature measurements in mountains, combined with the influences of local factors like cold air pooling and inversions, makes such quantification challenging. Dense networks of sensors with high temporal resolution are required to characterize well the patterns of surface temperature that occur over complex terrain [e.g., *Lundquist and Cayan*, 2007]. Since such observations are seldom available, empirical relationships between surface temperature and elevation are frequently exploited to aid in interpolating station data to make gridded fields.

[3]   For gridded analyses, surface temperatures are often assumed to decrease linearly with elevation, according to a temporally constant and spatially uniform lapse rate (decrease in surface temperature with elevation). For instance, *Maurer et al.* [2002] and *Hamlet and Lettenmaier* [2005] assume lapse rates of 6.5°C km^{-1} and 6.1°C km^{-1}, respectively, to create daily temperature grids for use in hydrological studies. Uniform and/or constant lapse rates have been used in a wide range of other studies, which typically assume lapse rates of 6.0 or 6.5°C km^{-1} [e.g., *Prentice et al.*, 1992; *Arnold et al.*, 2006; *Otto-Bliesner et al.*, 2006; *Roe and O'Neal*, 2010]. Sometimes authors justify these values as representative of the theoretical pseudo-adiabatic lapse rate [e.g., *Hamlet and Lettenmaier*, 2005], which can actually vary substantially due to its dependence on temperature and pressure (e.g., from about 3 to 9 °C km^{-1} for mid-latitude surface conditions). However, much more commonly authors offer no rationale for their use of the 6.0–6.5°C km^{-1} values. The use of these values is probably attributable in part to various sources that cite mean free atmosphere lapse rates in this range [e.g., *Wallace and Hobbs*, 2006]. The use of *mean* values may be problematic since they may not be representative of the atmosphere in a particular region in a particular season. Furthermore, using *free atmosphere* lapse rates for estimating surface conditions implicitly assumes that terrain and surface processes are unimportant in determining surface temperatures, which is only occasionally a good approximation [*Pepin and Seidel*, 2005]. For instance, in valley bottoms cold air pooling and temperature inversions can greatly alter the lapse rate [e.g., *Rolland*, 2003], and in mountain passes channeled cross-mountain flow can result in large local temperature anomalies [e.g., *Steenburgh et al.* 1997].

[1]Department of Atmospheric Science, University of Washington, Seattle, Washington, USA.
[2]Oregon Climate Change Research Institute, College of Oceanic and Atmospheric Sciences, Oregon State University, Corvallis, Oregon, USA.
[3]Department of Civil and Environmental Engineering, University of Washington, Seattle, Washington, USA.

[4] A number of observational studies using networks of temperature sensors have revealed that spatially uniform and temporally constant lapse rates of 6–6.5°C km^{-1} are not representative of actual surface conditions over the Appalachian mountains [Bolstad et al., 1998], the European Alps [Rolland, 2003], the Qinling Mountains of China [Tang and Fang, 2006], the central Rocky Mountains [Blandford et al., 2008], and Arctic glaciers [Gardner et al., 2009]. In all these regions mean surface lapse rates differ appreciably from the often-used 6–6.5°C km^{-1} values. Furthermore, observed surface lapse rates exhibit marked: (1) seasonal cycles, with amplitudes exceeding 2°C km^{-1} [Bolstad et al., 1998; Rolland, 2003; Tang and Fang, 2006; Blandford et al., 2008; Gardner et al., 2009]; (2) diurnal variability [Bolstad et al., 1998; Rolland, 2003; Tang and Fang, 2006; Blandford et al., 2008]; and (3) spatial variability, depending on the aspect of the slope [Tang and Fang, 2006], or location relative to valleys [Bolstad et al., 1998; Rolland, 2003].

[5] Several methods for temperature analyses go beyond the assumption of uniform and constant 6.0–6.5°C km^{-1} lapse rates. These approaches include specifying lapse rates that are uniform and constant, but are derived from station observations [e.g., Dodson and Marks, 1997], and specifying lapse rates that are spatially uniform but vary diurnally according to observations [e.g., Shamir and Georgakakos, 2006]. One of the most sophisticated statistical methods for analyzing mountain temperatures is the Parameter-elevation Relationships on Independent Slopes Model (PRISM) [Daly et al., 2002, 2008]. This method allows for both spatial and temporal variations in lapse rates based on station observations, and has been used for a variety of modeling [e.g., Elsner et al., 2009] and analysis [e.g., Weiss et al., 2009] studies.

[6] It is of utmost importance for societal planning in water resources, hydropower, agriculture, ecology, and other areas, to accurately quantify the present and future distribution of temperature over the landscape. This is particularly true in the field of mountain hydrology where the temperature grids of Maurer et al. [2002] and Hamlet and Lettenmaier [2005] have been used in the western US: to investigate the potential impacts of climate warming on snowpack and flooding [Bales et al., 2006], to identify climatic controls on snowpack trends [Hamlet et al., 2005], and even to diagnose human influences on regional climate [Bonfils et al., 2008]. Moreover, the importance of lapse rates extends far beyond hydrology; models of mountain glaciers [e.g., Otto-Bliesner et al., 2006; Roe and O'Neal, 2010], models of ecosystems [e.g., Prentice et al., 1992], and even geological reconstructions of terrain elevations from millions of years ago [e.g., Rowley and Garzione, 2007] utilize surface temperature lapse rates as important input parameters.

[7] Model errors associated with various lapse rate assumptions remain largely unquantified, but may be quite important. For instance, misrepresentation of the height of the 0°C isotherm is an error in temperature analyses that can have large consequences. Lundquist et al. [2008] show that each 100 m error in the estimation of the level where snow changes to rain, corresponds to a 5 % error in contributing area for runoff during a storm for the North Fork of the American River Basin in California, and White et al. [2002] show that runoff triples when the melting level rises by

2000 ft (610 m) in 3 of the 4 mountainous California watersheds they examined. Predictions from models of mountain glaciers have also been shown to be very sensitive to the assumed lapse rate [Otto-Bliesner et al., 2006; Gardner et al., 2009].

[8] In this paper we examine in detail annual mean and monthly varying lapse rates over the Washington Cascades mountains (Figure 1). The Cascades range in elevation from a few hundred meters to 4392 m MSL atop Mount Rainier. They have a large hydrologic sensitivity to climate warming [Bales et al., 2006], and have experienced the largest declines in spring snowpack [Mote et al., 2005] and shifts in timing of spring snowmelt [Stewart et al., 2005] in the western US. Previous characterizations of temperature lapse rates in the Cascades have been limited. Dodson and Marks [1997] quantified mean lapse rates over the Cascades, but only as a part of a much larger analysis domain. Rasmussen [2009] examined lapse rates and their seasonality in the northern Cascades, but only used data from a single pair of stations.

[9] Our analysis extends beyond the scope of previous studies by using a synthesis of several observational data sets and a regional weather prediction model, presenting long term mean statistics and also statistics from two recent periods when we collected high resolution measurements. Our results from the Cascades may be considered a case study in how various data sets in any region can be used to determine the most reliable lapse rate for hydrological and ecological model simulations. Our findings reveal that the canonical mean lapse rate (6.5° C km^{-1}) poorly characterizes the Cascade climate, and furthermore, variations in the lapse rate (particularly geographic variations) can be of considerable importance to regional hydrology.

2. Data and Methods

2.1. COOP Stations

[10] We obtained monthly mean daily maximum and minimum temperatures (Tmax, Tmin) for all National Weather Service Cooperative (COOP) weather stations in Washington Climate Divisions 5 (western Cascades) and 6 (eastern Cascades), a total of 129 stations, from the Western Regional Climate Center (www.wrcc.dri.edu). The distribution of COOP stations appears quite dense (Figure 1), but most stations at middle and high elevations were discontinued by 1980. Although high elevation coverage is limited, we focus on COOP station data because it offers quality controlled data from a stable network over an extended time period. We performed least squares linear regression to derive lapse rates using monthly and annual means of Tmax and Tmin for each station. To compute annual means we required all months be available. For Paradise (at 1650 m on Mount Rainier, Figure 2), data in November 2006 were missing, owing to heavy storm damage. Missing Paradise data were estimated from measurements taken by a collocated iButton sensor (see below) using linear regression.

[11] To ensure that our calculation of lapse rates is robust, we investigated the annual mean lapse rates for a range of: (1) periods of record (starting years from 1939 to 1969), (2) thresholds for required number of years of valid station data in a 30-year period (from 14 to 30 years), and (3) minimum station elevation used (from 0 to 300 m). In most cases,
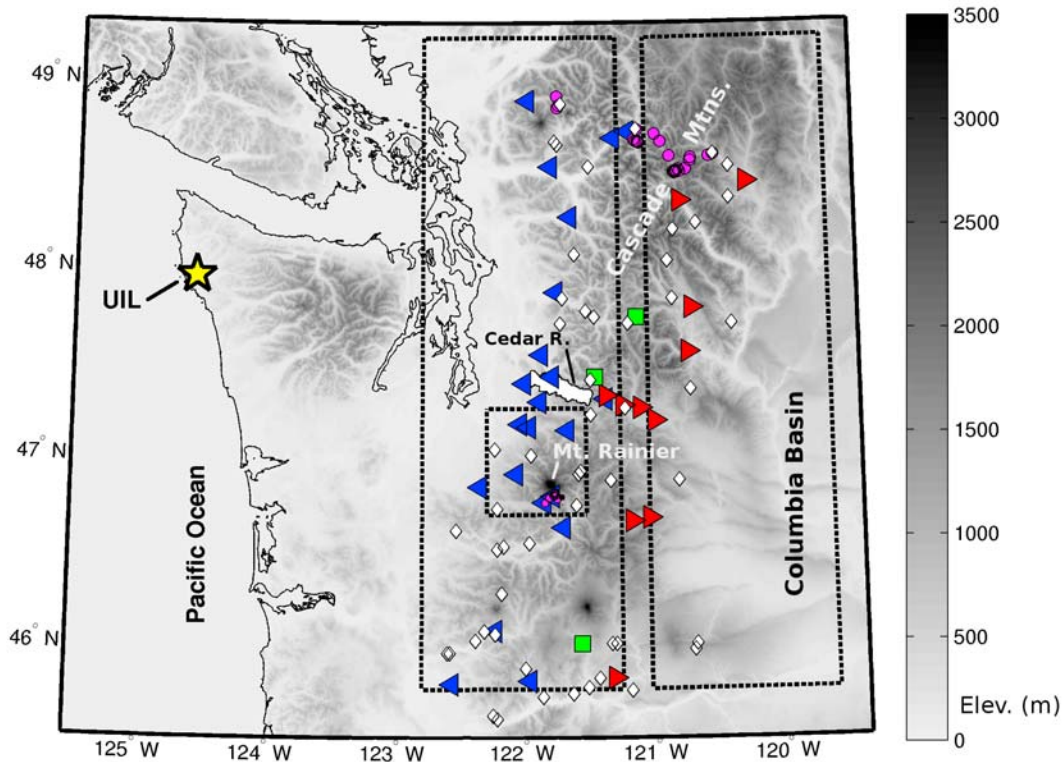
Figure 1. Map of WA Cascade study region. The location of radiosonde launches is shown with a yellow star (labeled UIL). COOP stations used in this study are indicated by left-pointing blue triangles for windward side and right-pointing red triangles for lee side; three COOP stations indicated with green squares are used for both lee and windward side calculations. Other COOP stations that were not used are shown as small white diamonds. Locations of iButtons deployed for this study are shown with magenta circles. Dashed rectangles show the Rainier (small box), windward (western), and leeward (eastern) domains used for analysis of MM5 and PRISM grids. The Cedar river basin is colored white. Important geographic features are labeled. Grey scale indicates elevation in meters.

as long as there were at least 10 stations, any combination of requirements about missing months, period of record, or minimum station elevation used, produced essentially the same annual mean lapse rates (to within $0.2°$ C km^{-1}). We chose the period 1949–1968, a minimum elevation of 50 m, and minimum number of valid years of 19 (a combination that produced the same maximum and minimum lapse rate as the average computation for all combinations of choices with at least 10 stations). These stations have a variety of exposures relative to the surrounding terrain and many of the low elevation valley stations are likely to at least occasionally reside in localized cold air pools. Considering sampling uncertainty in the lapse rate regression, the 95% confidence interval on the estimate of the COOP annual mean lapse rates is ±0.9 and ±1.0 °C km^{-1} for 1949–1978 maximum and minimum temperatures (±0.9 and ±1.2°C km^{-1} for 2006–2007).

2.2. High-Resolution Transects: iButtons

[12] We deployed a dense network of Maxim iButton temperature sensors on the south side of Mt. Rainier (Figures 1and 2) for 2006–2007 and in the northern Washington Cascades mountains (Figure 1) for 2007–2008. Before and after deployment all sensors were placed in an ice bath to verify their accuracy of recording 0°C and were also compared when taking room temperature measurements to

verify consistent performance between sensors. They all performed better than ±0.2°C.

[13] In the field the iButtons were placed in simple radiation shields made from plastic funnels and were deployed in stands of evergreen trees to provide additional shading from solar radiation. Sensors were hung in trees, as high as possible — from 2 m to 8 m above ground level (AGL) — to keep them above the snowpack and near-surface temperature inversions. Our deployment methodology follows *Lundquist and Huggett* [2008], who show that when deployed in dense stands of trees iButton measurements agree well with reference measurements from more traditional instrumentation. The iButton data were subjected to additional quality control to remove anomalous spikes in recorded temperature associated with brief periods when rays of solar radiation penetrate the forest canopy and strike the sensor; however the seasonal mean measurements were minimally affected by this correction. The height of iButtons above the snow surface varies as a function of the snow depth, which is unknown. This represents a fundamental source of uncertainty in the iButton measurements (and most other temperature measurements in high snowy terrain), particularly if the snow height approaches the sensor height and the sensor is exposed to near-surface temperature inversions. However,
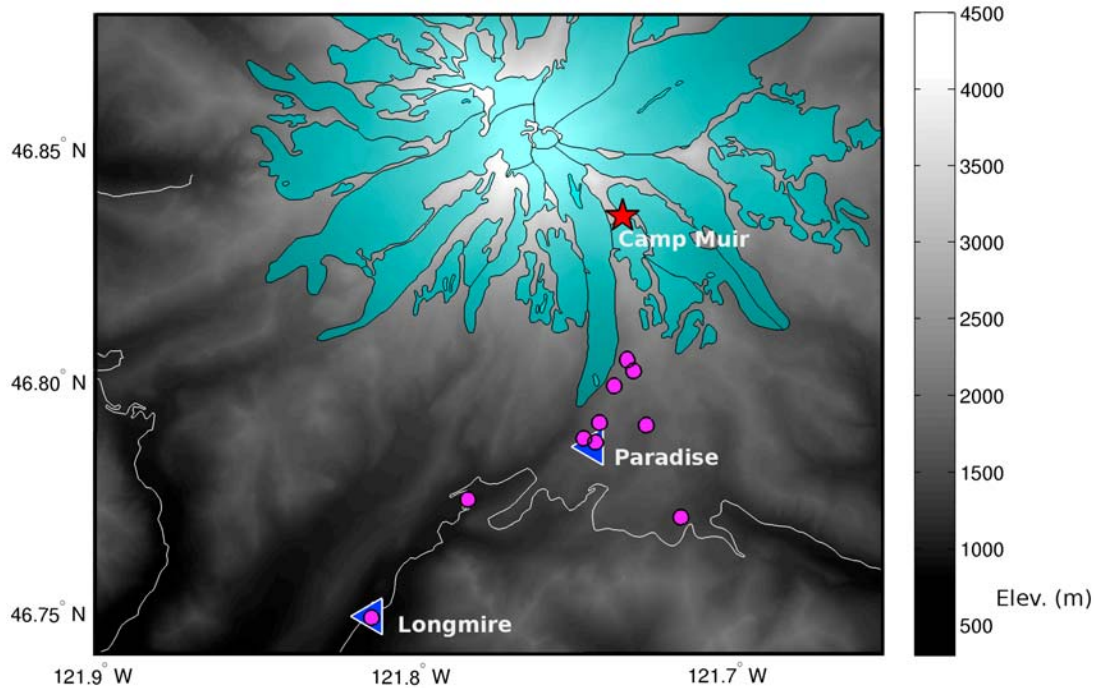
Figure 2. Map of 2006–2007 Rainier field study region. Locations of iButton temperature sensor deployments are shown with magenta circles. The Camp Muir station is indicated with a red star. The Longmire and Paradise COOP stations are indicated with blue triangles. Glaciers on the mountain are shaded in cyan. Major roads are shown with grey lines. Grey scale indicates elevation in meters.

we minimized this uncertainty by hanging the sensors high above the expected maximum snow depth.

[14] At Mt. Rainier (elevation 4392 m), we installed 12 iButtons in stands of trees on October 1, 2006, along an 8-km transect from the COOP station at Longmire (840 m) to the highest stand of trees at 2100 m (Figure 2). They were hung 2–5 m AGL in trees. On August 30, 2007 we retrieved 10 of the iButtons (one was lost and one was so wind-battered that we were unable to recover data from it). One sensor became snow covered from Dec–May, and accordingly its data were omitted from the analysis. iButtons agreed well with COOP instrumentation at the two site where they were collocated in nearby trees: root-mean-squared differences for monthly mean temperatures were 0.9°C at Paradise and 0.4°C at Longmire, and annual mean differences were less than 0.2°C at both sites.

[15] In the northern Cascades, we installed 21 iButtons in an approximate east-west transect crossing the crest of the Cascades. They were deployed on September 7–10, 2007, and retrieved August 1, 2008 (Figure 1). They were hung 1.8–7.9 m AGL in dense stands of trees. The horizontal and vertical range of measurement sites was considerably greater than at Mt Rainier: 47 km and from 360 to 2120 m. All data from all sensors were recovered.

[16] The iButtons recorded temperatures every hour. We used the hourly measurements to calculate daily mean temperatures, and then calculate daily, monthly, and annual mean lapse rates (using linear regression, as for the COOP stations). We also recalculated the iButton lapse rates with additional data from a high permanent station at Camp Muir on Mt. Rainier (3070 m; see Figure 2). Unfortunately, many

missing hours of data from this site prevented us from using it in the investigation of annual means or seasonal variability. However, including Camp Muir as a test, using the 3 months when the most data were available (months that had at least 24 days with at least 16 hourly observations), changed the monthly lapse rates by only 0.1°C km^{-1} on average, and by 0.3°C km^{-1} at most. Considering scatter about the temperature-elevation regression line, the 95% confidence interval for the estimate of the iButton annual mean lapse rates is ±0.6°C km^{-1} for Mt. Rainier and ±0.7°C km^{-1} for the North Cascades.

2.3. Radiosondes

[17] We analyzed free air lapse rates from radiosonde measurements at Quillayute on the Washington coast (marked UIL in Figure 1), obtained from the University of Wyoming sounding archive (http://weather.uwyo.edu/upperair/sounding.html). This data set provided twice daily (00 and 12 UTC, 16 and 04 LST) temperature profiles for 1973–2007. We analyzed both the whole 34 year period, and also isolated the Mount Rainier (2006–2007) and North Cascade (2007–2008) iButton observing periods, for comparison. For each sounding used, the temperature measurements were linearly interpolated to a regular 100 m vertical profile before the analysis, and monthly mean lapse rates from the 0.5–2.5 km layer were calculated by linear regression. Mean soundings for each month were constructed by averaging the temperatures from all available soundings. For 1973 to 2007, 93% of the 00 and 12 UTC soundings were available and complete enough for use in the analysis. For the north Cascades and Rainier observing periods 94 % and

92 % of possible soundings were present. A cursory analysis of soundings associated with mountain precipitation events was also conducted by identifying "wet" soundings for separate analysis. Since defining region-averaged precipitation from sparsely spaced gauges is not straightforward we chose to simply focus on soundings with conditions typical of mountain precipitation events in the region [e.g., *Smith et al.*, 2005; *Minder et al.*, 2008]: 0.5–2.5 km wind directions between 140 and 320 degrees and relative humidity greater than 80 %.

2.4. MM5 Forecasts

[18] We also analyzed surface lapse rates from operational high resolution numerical weather prediction model simulations over the region. From 1997 until mid-2008, the Northwest Regional Modeling Consortium at the University of Washington ran the fifth generation Penn State-National Center for Atmospheric Research Mesoscale Model (known as the MM5) [*Grell et al.*, 1995] over the Pacific Northwest [*Mass et al.*, 2003]. They ran the MM5 at 4 km horizontal resolution twice daily (initialized at 00 and 12 UTC, 16 and 04 LST). The model was run with a full suite of sophisticated physical parameterizations for atmospheric radiation, surface fluxes, convection, clouds and precipitation, etc. MM5 solves for the surface temperatures by considering the physical processes contributing to the surface energy budget including radiative, turbulent, advective, ground, and latent heat fluxes. A full description of the model runs can be found at: http://www.atmos.washington.edu/mm5rt/mm5info.html.

[19] By piecing together hourly output from forecast hours 12–24 of consecutive archived MM5 forecasts, we created a time series of daily averaged 2 m air temperatures predicted by the model at each grid point. The model grids were analyzed for the 2006–2007 Mount Rainier observing period for comparison with observations. The MM5 output was analyzed over three domains (Figure 1): roughly the windward (western) and lee (eastern) sides of the Washington Cascades, and Mount Rainier and its immediate surroundings. The Rainier domain is substantially larger than the iButton field study region so that enough MM5 grid points can be included to attain good regression statistics. Additional calculations with a smaller domain (about one-quarter smaller in area, focused more tightly around Rainier's peak) gave lapse rates that differed by less than 1°C km^{-1} in any given month and less than 0.1°C km^{-1} in the annual mean. For each region only gridpoints above 200 m elevation were used to exclude the relatively flat lowlands and focus on mountainous areas (Figure 1). Daily and monthly mean lapse rates were calculated for each region, using linear regression. The elevation grid used by MM5 was used for the regression. Since region-averaged precipitation could be readily diagnosed from the model, output forecasts with average precipitation > 2 mm 12 h^{-1} were identified to characterize "stormy" lapse rates for separate analysis.

2.5. PRISM Analysis

[20] The Parameter-elevation Relationships on Independent Slopes Model (PRISM) [*Daly et al.*, 2002, 2008] (www.prism.oregonstate.edu) is a statistical algorithm that objectively combines monthly- and annual-mean data from essentially all available stations to create high resolution gridded analyzes. PRISM uses localized linear regression of temperature and elevation to define lapse rates that are then used to construct grids for average daily maximum and minimum temperatures. This approach allows surface lapse rates to vary seasonally and spatially, and to differ from the free air. Before the temperature-elevation regression is calculated, stations are assigned weights according to their "physiographic similarity" to the grid cell of interest (in terms of aspect, proximity to water bodies, expected position in the boundary layer, etc.). Through this weighting procedure PRISM attempts to account for the effects on temperatures of cold air pooling, low-level inversions, and water bodies [*Daly et al.*, 2008]. The station data used are subjected to additional quality control before the PRISM interpolation [*Daly et al.*, 2008]. At high elevations in the Cascades the PRISM analysis relies primarily on observations from the SNOTEL (www.wcc.nrcs.usda.gov/snow/) and RAWS (www.fs.fed.us/raws/) networks. PRISM also includes COOP data, and thus it does not represent a completely independent data source.

[21] We calculated long term mean lapse rates from the 1971–2000 PRISM monthly normals, gridded at 800 m resolution. We also analyzed the standard monthly PRISM data, gridded at 4 km resolution, for the 2006–2007 Mount Rainier observing period. We approximated monthly mean PRISM temperatures by averaging monthly mean Tmax and Tmin together, then analyzed the PRISM grids using the same methods and domains as for the MM5 data. The elevation grids used in the regression came from the PRISM data set and were originally derived from the National Elevation Data set (http://gisdata.usgs.gov/NED/) as described by *Daly et al.* [2008].

3. Results

[22] The data sources listed above describe temperature variability over different domains at different resolutions, and hence the results should not be expected to match exactly. Since they each have their owns strengths and weaknesses the data sets complement each other and together provide a more complete view of temperature variability in the Cascades. The COOP data span the longest time period and a large region, but the highest COOP station (Paradise) is at an elevation of only 1650 m. The iButtons provide high resolution in time (hourly) and space (100 m or less in the vertical), and extend to somewhat higher altitude (2120 m) but were only deployed for a year and only in two small areas of the Cascades. The radiosonde measurements are taken twice daily, with high vertical resolution, and extend back for several decades, but they sample the free air, not the surface, and only at one location over 100 km from the Cascades. Output from MM5 simulations is uniformly distributed in space and time, but even at 4 km resolution, the grid box elevations reach only about 2500 m at Mt Rainier (actual peak elevation 4392 m). Furthermore, MM5 lapse rates are model predictions and thus subject to model biases. Finally, the PRISM analysis incorporates data from all available observational networks, but has only monthly resolution, relies on various assumptions in the interpolation procedure, and may be subject to sizable errors where station observations are sparse.
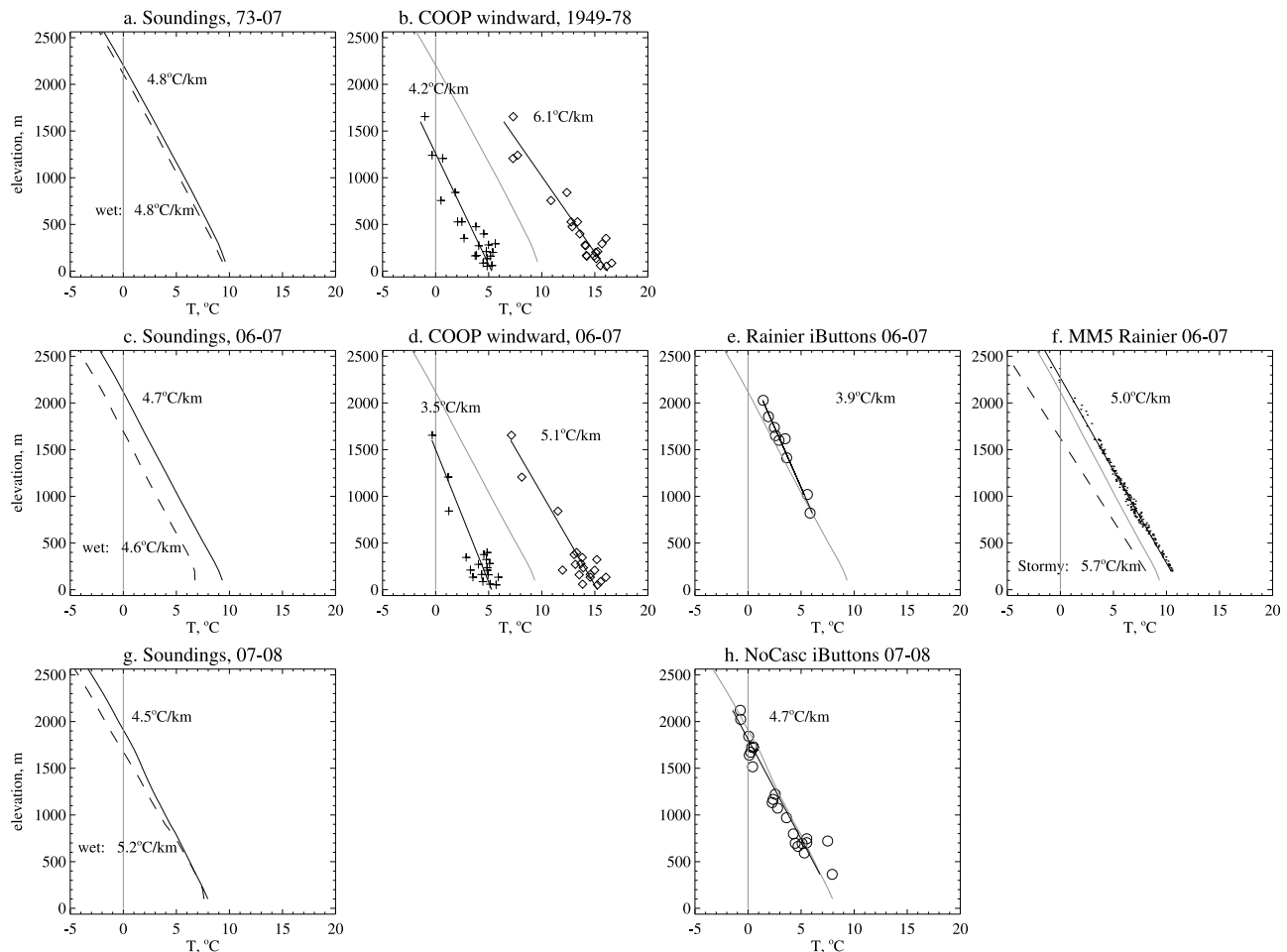
Figure 3. Mean profiles and lapse rates for various data sources and periods. (a–b) Long-term means for the periods indicated. (c–f) The 2007 water year. (g–h) The 2008 water year. For the UIL soundings (Figures 3a, 3c, and 3g), annual mean soundings are shown for all (solid line) and "wet" (dashed line) conditions. For COOP data (Figures 3b and 3d), mean temperatures and linear fits are shown for both daily maximum (diamond) and minimum (+) temperatures. For iButton data (Figures 3e and 3h), data from individual sensors are shown with o's as well as linear fits (black line). For the MM5 grids from the Mount Rainier domain (Figure 3f), the mean temperatures at individual MM5 grid points are shown as dots, and linear fits are shown for all data (solid line) and "stormy" days (dashed line). In each row the mean sounding from the leftmost panel (Figures 3a, 3c, and 3g) is repeated (as a grey line) in the other panels (Figures 3b, 3d–3f, and 3h) for reference.

3.1. Annual Means

[23] Figure 3 shows annual mean temperatures and lapse rates for our data sets. Annual mean lapse rates vary from 3.9°C km^{-1} for the Rainier iButtons to 5.7°C km^{-1} for MM5 during storms in the same year, and no data set shows annual-mean lapse rates of daily-averaged temperatures as large as 6°C km^{-1} (although annual mean lapse rates of daily *maximum* temperatures in COOP data reach 6.1°C km^{-1}; see Figure 3b). In the mean soundings (Figures 3a, 3c, and 3g), "wet" days are slightly cooler than all days, but the lapse rates are about the same. Sounding lapse rates are similar in 2006–2007 and 2007–2008 when calculated using all data, and are 0.6°C km^{-1} higher on wet days in 2007–2008 than in 2006–2007 (Figures 3c and 3g).

[24] The COOP climatology shows significantly greater annual mean lapse rates for the daily Tmax than Tmin

(6.1°C km^{-1} versus 4.2°C km^{-1}) for 1949–1978 (Figure 3b). COOP Lapse rates for 2006–2007 were smaller than the climatological mean (Figure 3d). For 2006–2007 the "mean" COOP lapse rate (from the average of Tmax and Tmin) was 4.3°C km^{-1}, quite close to the mean lapse rate from the 2006–2007 soundings, 4.7°C km^{-1}.

[25] PRISM 1971–2000 normal grids over the windward slopes (not shown) have annual mean lapse rates very similar to the COOP stations for Tmin (4.1°C km^{-1}), but have smaller values for Tmax (4.8°C km^{-1}). Thus, the inclusion of other observational networks (e.g., RAWS and SNOTEL) and station-weighting techniques in the PRISM analysis does result in somewhat different lapse rates then those attained from the relatively sparse COOP coverage alone.

[26] For the iButton data, the lapse rate for the Rainier domain during 2006–2007 (Figure 3e) is 3.9°C km^{-1}. This value is smaller than the lapse rate from the soundings, and

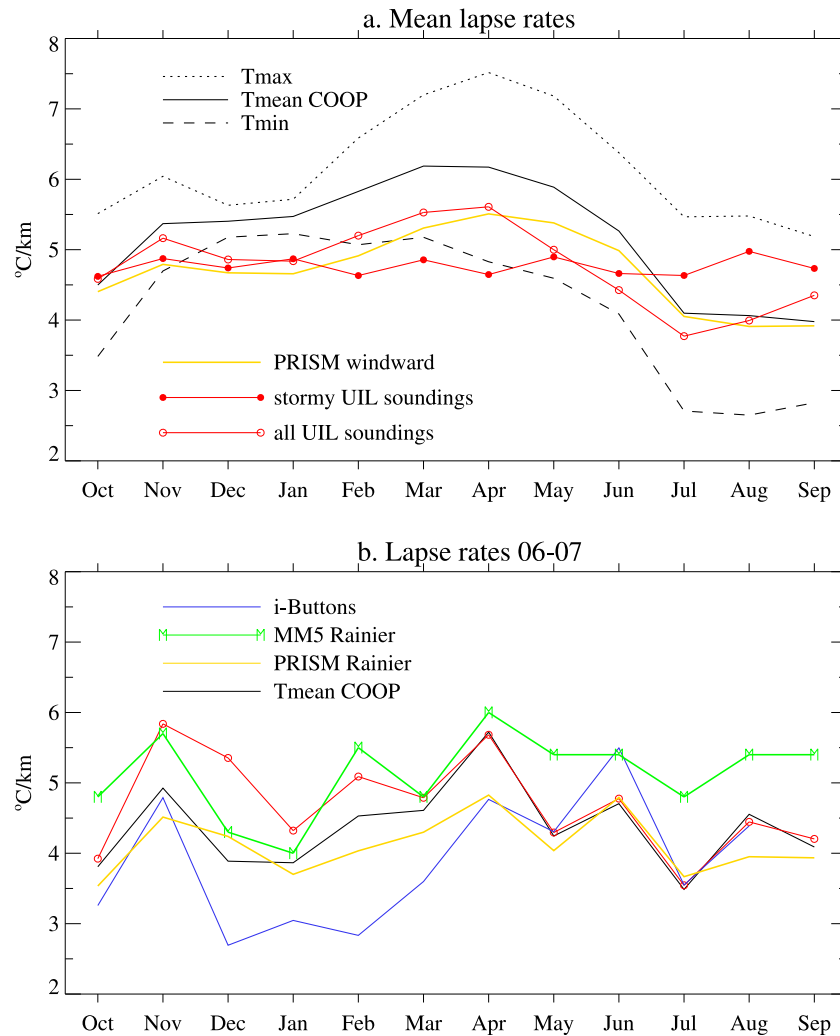## a. Mean lapse rates

b. Lapse rates 06-07

Figure 4. Mean seasonal cycle of lapse rates: (a) long-term mean from windward COOP stations (Tmax, Tmean, Tmin), PRISM (Cascades windward domain, 800 m climatological grids), and UIL sounding data (all soundings, and "stormy" soundings), as indicated in legend; (b) 2006–07 season, from Mount Rainier iButtons, MM5 and PRISM grids from the Rainier domain, and windward COOP station Tmean.

accordingly the iButtons are warmer at high elevations than the soundings, an unexpected result for an isolated peak where high elevations are well-exposed to the free air, only rarely under calm conditions dominated by local surface energy balance. In contrast, the iButtons in the northern Cascades in 2007–2008 (Figure 3h) have a mean profile very similar to that of the soundings during the same period.

[27] Mean MM5 lapse rates for the Rainier region in 2006–2007 (Figure 3f) show somewhat higher values than the sounding, iButton, and mean COOP observations: 5.0°C km^{-1}. The MM5 lapse rate during stormy conditions is 5.7°C km^{-1}, larger than the mean value.

3.2. Seasonal Variability

[28] The seasonal cycle of long term monthly-mean lapse rates (from COOP, PRISM, and the UIL soundings) is shown in Figure 4a. While the magnitudes of the lapse rates are somewhat different in the various data sets, the seasonal variability is similar. The lapse rates change appreciably

through the year, with largest lapse rates for Tmax in spring and smallest lapse rates for Tmin in summer. "Wet" soundings had nearly constant lapse rates, between 4.5 and 5°C km^{-1}. In all months lapse rates of COOP Tmax exceed lapse rates of Tmin. The seasonality of lapse rates from all soundings closely resembles that from the COOP observations and PRISM grids, suggesting that the mean regional surface lapse rates are largely determined by region-wide air mass characteristics as represented by the soundings.

[29] Since low-level marine stratus clouds can strongly influence the temperature profiles in the coastal region, but would not be expected to affect temperatures over the Cascade mountains, the coastal UIL soundings may at times poorly represent the free air abutting the Cascades. Figure 5a plots the seasonal cycle of UIL lapse rates for different layers to examine how strongly low-level features such as marine clouds may affect results. When only the 0.5–1 km layer is considered, the summertime (Jul–Aug) lapse rates are strongly reduced, consistent with the frequent summer-
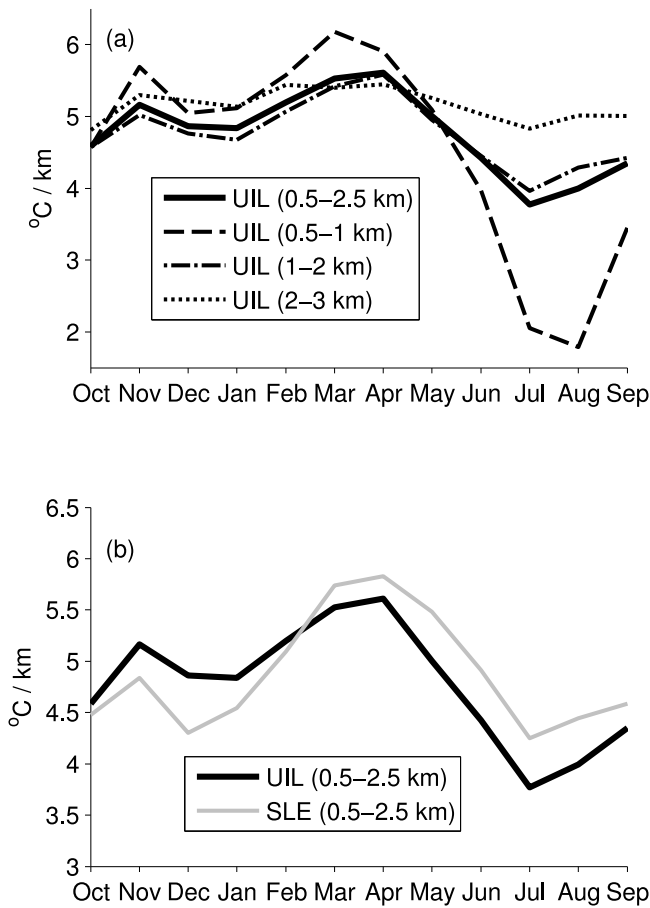
Figure 5. Mean seasonal cycle of sounding lapse rates calculated from: (a) various layers of the UIL sounding (as indicated in legend) and (b) 0.5–2.5 km layers of the UIL and SLE soundings.

time occurrence of marine stratus that reduce near-surface temperatures and are often associated with temperature inversions. This summertime anomaly is much reduced when the 1–2 km layer is used. Nearly all seasonality is eliminated by using the 2–3 km layer, but this layer is above most of the Cascades topography. The 0.5–2.5 km lapse rates used throughout this study follow most closely the 1–2 km values, suggesting that they are not strongly influenced by near-surface coastal processes. Figure 5b further examines this issue by comparing the seasonality from the UIL sounding with that from the Salem sounding (SLE, also from 1973–2007) located about 360 km south of UIL, over 50 km inland from the Pacific Coast, and separated from the Pacific by the ~500 m tall Oregon Coastal range. That the SLE and UIL soundings show very similar seasonal cycles indicates that the 0.5–2.5 km UIL climatology is indeed representative of regional-scale free air conditions without a strong influence of coastal effects.

[30] The seasonal cycle for the 2006–2007 Mount Rainier study period (from COOP, PRISM, MM5, UIL, and the iButtons) is shown in Figure 4b. Month-to-month variations are larger for this single year than for the multi-year climatologies. Again, there is good correspondence among the various data sets despite the different domains and quantities represented. All show a relatively large lapse rate in

November as well as in April. Much smaller lapse rates are shown for October, January, and July. The closest correspondence is between the UIL sounding and COOP data, again suggesting that seasonal variations in region-wide surface lapse rates are strongly controlled by the free air temperature profile. The measurements with the smallest spatial scale, the iButtons, show the weakest correspondence with the soundings, suggesting that on the scale of an individual mountainside local factors remain important in addition to the regional air mass conditions.

3.3. Geographic Variability: Windward Versus Lee

[31] To investigate geographic variability in lapse rates, we compare the lapse rates on the windward (west) and leeward (east) sides of the Washington Cascades (Figure 6). In both the long term PRISM climatology and the 2006–2007 PRISM data the leeside shows a larger seasonal cycle with a different phasing than the windward side (Figure 6a). In the lee the lapse rates vary by about 4°C km^{-1}, greatest in May–Jul and smallest in Dec–Jan. The lee side seasonality is similar to that found by *Rasmussen* [2009] using a single pair of stations in the northeastern Cascades. This lee side
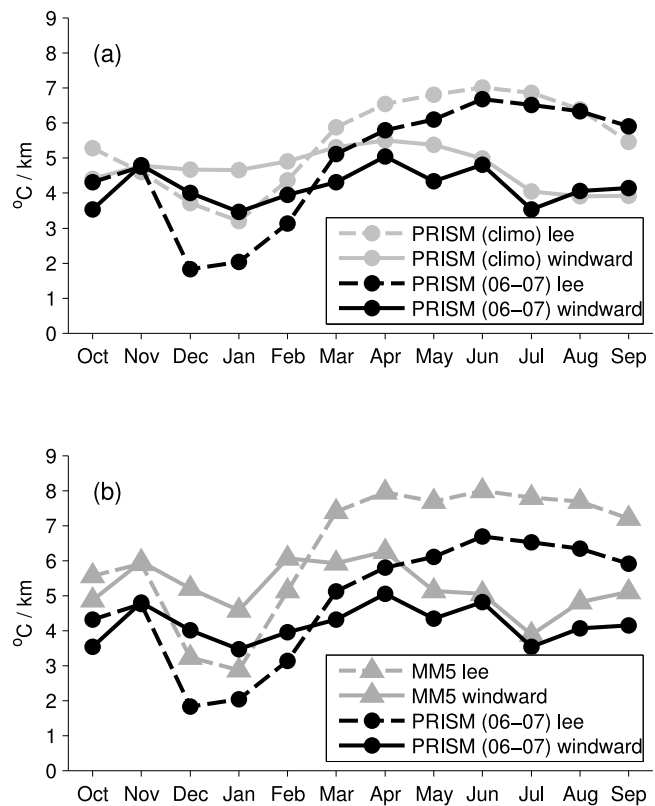

Figure 6. Comparison of lapse rates for the Cascade windward and lee domains. (a) Seasonal cycle from the long-term PRISM climatology (1971–2000, with 800 m horizontal gridding) for the windward (grey solid) and lee (grey dashed) domains as well as for the 2006–2007 season from PRISM (with 4 km horizontal gridding, plotted in black). (b) Seasonal cycle for 2006–2007 from PRISM (as in Figure 6a), and MM5 windward (grey solid) and lee (grey dashed) domains.
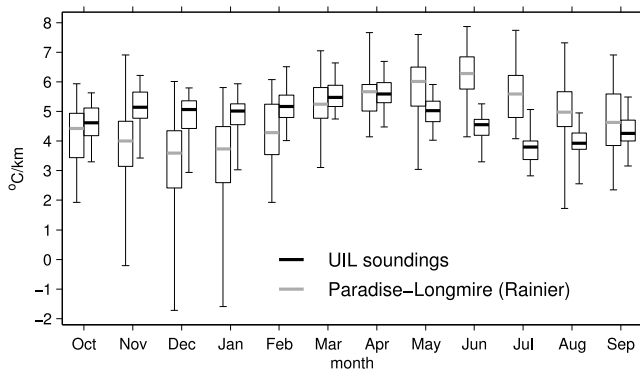
Figure 7. Year-to-year variability in monthly-mean lapse rates. Thick horizontal lines show the month's median lapse rate calculated using the UIL soundings from 1973–2007 (black) and the Paradise-Longmire station pair from 1948–2006 (grey). Boxes show the inner-quartile range, and the whiskers show the full range of the data.

seasonality contrasts with the more muted seasonal cycle on the windward side (about 1°C km^{-1}), with largest lapse rates in Mar-Mayand lowest in Jul–Sep. These differences between windward and lee side lapse rates are apparent for 2006–2007 in MM5 as well (Figure 6b), with MM5 showing higher lapse rates than PRISM, but similar seasonal cycles.

[32] Results from lee side COOP data are similar (not shown), but lapse rates in COOP minimum temperature are problematic because the stations on the east slopes of the Cascades are mainly in deep valleys (Figure 1), potentially subject to strong localized cold air pooling. While biases of the lee side COOP stations may affect the PRISM analysis (although PRISM attempts to account for cold air pooling [*Daly et al.*, 2008]), the agreement between the MM5 and PRISM leads us to conclude that the windward versus lee side differences in lapse rates are a robust feature.

[33] Low lee side lapse rates can result from the pooling of cold continental air in the Columbia Basin (Figure 1) and the damming of cold air against the eastern slopes of the Cascades [e.g., *Bell and Bosart*, 1988; *Steenburgh et al.*, 1997; *Whiteman et al.*, 2001]. Both of these phenomena occur primarily in the wintertime, and result in an accumulation of cold air at low elevations in the lee that greatly decrease lapse rates, often resulting in temperature inversions. *Whiteman et al.* [2001] developed a climatology of Columbia basin cold pool events by identifying periods >18 h with low wind speeds and temperature inversions. This climatology shows the greatest frequency of cold pools in Dec and Jan. Thus these events are likely responsible for the minimum in lee side lapse rates found in the same months (Figure 6). Additionally, clear winter nights with strong radiative cooling in the lee of the Cascades may lead to more cold air drainage into valleys, resulting in locally reduced lapse rates [e.g., *Rolland*, 2003]. Such differences in lapse rates across mountains are likely a common feature for ranges that separate maritime and continental climatic zones.

3.4. Year-to-Year Variability

[34] Estimating year-to-year variability requires a long and consistent data set. Unfortunately the shortness of the

MM5 and iButton data sets, and the network changes in the COOP and PRISM data sets mean the UIL soundings likely offer the only good regional-scale measure of interannual lapse rate variability.

[35] We examine the year-to-year regional variability by analyzing the distribution of monthly mean lapse rates calculated from the 35 yrs of UIL sounding data. Figure 7 shows the median, inner-quartile range (IQR), and full range of UIL lapse rates. Typical variations in the lapse rate, as measured by the IQR, are modest; the IQR varies from 0.54°C km^{-1} (Jun) to 0.93°C km^{-1} (Oct). The full range of monthly mean lapse rates is substantially larger. It is largest in the late-fall and winter months (Nov–Feb, peaking at 2.9°C km^{-1}), and smallest in the summer (Jun–Aug) (Figure 7).

[36] For comparison we also plot the distribution (median, IQR, range) of monthly-mean lapse rates calculated from the pair of COOP stations on Mt Rainier (Longmire and Paradise; see Figure 2). All available monthly mean data from 1948–2006 were used, and the lapse rates were calculated simply as the difference between the station temperatures divided by the elevation difference (Figure 7). Comparing results from the station pair with the regional signal represented by the soundings shows a similar mean lapse rate and a similar increase in lapse rate variability in wintertime, but the similarities end there. The seasonal cycle from the station pair is distinctly different, indicating the largest lapse rates in months when the sounding lapse rates are at some of their lowest values. Additionally, the station pair also shows much larger year-to-year variability of the monthly-mean lapse rate, even showing some years with negative values in Dec–Jan. These differences may be attributable to local aspects of climate around these stations such as the seasonal cycle of snow cover, cold air pooling at Longmire (a valley site), and/or orographic clouds unique to Mount Rainier.

3.5. Day-to-Day Variability

[37] To reveal variability in lapse rates on day-to-day timescales we plot, for each month of 2006–2007 field season, the median and IQR of daily lapse rates from the iButton and MM5 in Figure 8a. The observations show large day-to-day variability in the lapse rates, with the IQR exceeding 4°C km^{-1} in Oct and Aug. The MM5 shows much less day-to-day variability than the iButtons in months with large observed variability (the largest IQR is about 2°C km^{-1}), but shows similar amounts of variability in months with small observed variability. The reduced variability in the MM5 relative to the iButtons may be due to model bias, or to the more region-averaged nature of the MM5 data compared to the more localized iButton observations.

[38] We also compare MM5 modeled day-to-day lapse rate variability on the windward and lee slopes for 2006–2007. The windward slopes show similar variability to the Rainier domain. From late spring through fall the lee slopes also have similar variability, however the lee side variability is greatly enhanced in the winter months (Dec–Mar), with Dec and Jan exhibiting IQRs of over 4°C km^{-1}. This large wintertime variability is likely associated with events where
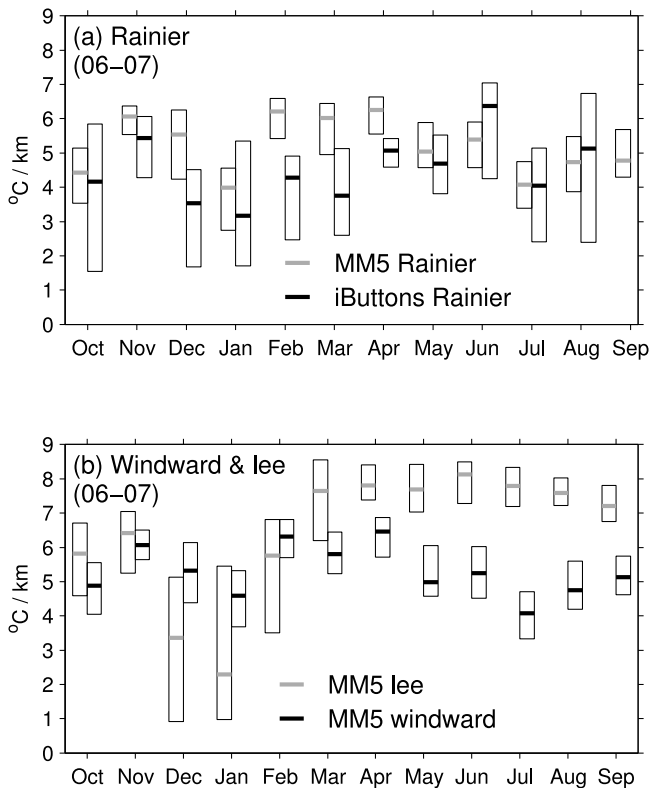
Figure 8. Day-to-day variability in lapse rates for the 2006–2007 field season. (a) Median (bold line) and inner-quartile range (IQR, shown with boxes) of daily lapse rates for each month from the MM5 (grey) and iButton (black) data over the Rainier domain. No iButton data is shown for Sept since sensors were not deployed during that month. (b) Median and IQR (plotted as in Figure 8a) from MM5 data over windward (black) and lee (grey) domains from 2006–2007.

cold continental air accumulates against the lower lee slopes, as discussed in section 3.3.

4. Implications for Hydrological Modeling

[39] Having characterized how the surface lapse rates in the Cascades differ from the typically assumed value of 6.5°C km^{-1} we now proceed to investigate the implications of our results for hydrological modeling. We first turn to the results of *Casola et al.* [2009], who estimated the sensitivity of the western Washington Cascade snowpack to climate warming using a simple geometrical model and a sophisticated hydrological model. Both models assumed a lapse rate of 6.5°C km^{-1} and estimated a 22–23 % loss of April 1st snow water equivalent per degree of warming (when precipitation changes were neglected). However, changing the lapse rate in their geometrical model to 5.0°C km^{-1} (a value more representative of actual lapse rates in the region) increases this sensitivity to a 30 % loss of snowpack per degree of warming, a major change. Projections of future snowpack and streamflow for this region from other models with the same assumption built in [e.g., *Snover et al.*, 2003] may be similarly affected by the adjustment to the true surface lapse rate.

[40] We further highlight the importance for hydrology of correctly characterizing surface temperatures by presenting a simple model for streamflow in the Cedar River basin of the Washington Cascades (outlined in Figure 1). The model is forced by the climatological daily-mean temperature and precipitation from a single low elevation station in the basin (the Cedar Lake COOP station: 47.25°N, 121.44°W, elevation 475 m). The basin is divided into 8 elevation bands (each covering 200 m of elevation) and precipitation is distributed uniformly over the basin. For one set of experiments, temperatures for each elevation band are determined from the station data by using constant lapse rates of 6.5, 5, and 4 °C km^{-1}. For another pair of experiments the climatological mean seasonal cycles of PRISM lapse rates from the windward and lee sides are used (Figure 6).

[41] The SNOW-17 model (used in operational river forecasting) [*Anderson*, 1976] was applied to determine the accumulation and melting of snow. At temperatures < 0°C the model assumes precipitation falls entirely as snow, and at temperatures > 1°C it assumes only rain. A mixture of rain and snow falls at intermediate temperatures. For snowmelt the model uses an energy balance approach during rain-on-snow events and a degree day approach during non-precipitating days. Snowmelt and rain water from SNOW-17 were entered into a linear reservoir model to simulate streamflow, accounting for basin storage delays. The model performs a convolution integral of the snow model output with a response function, $\frac{h}{\sum h}$, where $h = exp(-t/\tau)$, $\tau = 31.3$ days, and t ranges from 1 to 18 days (following the formulation given by *Dooge* [1976]).

[42] The three hydrographs associated with the three assumed constant lapse rates (Figure 9a) all show a maximum associated with rainfall in the autumn, a minimum associated with snowfall in the winter, a larger maximum associated with springtime rainfall and snowmelt, and a late summer minimum when the snow has melted and little precipitation falls. However, large differences in the shape of the hydrograph occur when the assumed lapse rate is varied. For smaller lapse rates, high elevations are warmer, and thus more precipitation falls as rain (increasing the autumn peak flow, and early spring flow). Furthermore, with smaller lapse rates less precipitation accumulates as snow, and the snow that does accumulate melts faster due to warmer high elevation temperatures (causing reduced late spring flow and a shift of the springtime hydrograph). The opposite occurs when lapse rates are increased. A particularly dramatic effect is the change in the start of the summer melt (the date at which the snowpack begins its nearly monotonic decline): it is shifted a full month earlier when the lapse rate is changed from 6.5 to 4° C km^{-1}.

[43] Hydrographs associated with seasonally varying lapse rates are shown in Figure 9b. Seasonality has little effect when windward lapse rates are used, since there are only modest seasonal variations. Seasonality is much more important when lee side lapse rates are used. Because the leeward slope has much smaller lapse rates in January (3 to 4° C km^{-1}) high elevations are warmer and receive more liquid precipitation. However, because lee side lapse rates become much larger in the spring (around 7° C km^{-1}), the snow that does fall takes longer to melt. The net result is increased flow in winter and summer, but decreased flow in
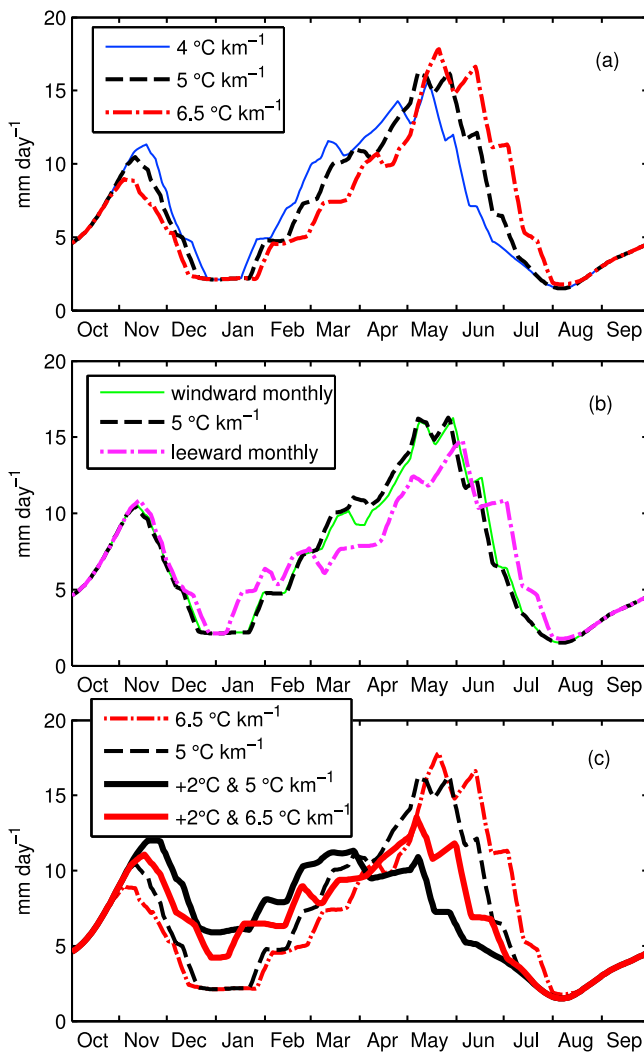
Figure 9. Hydrographs for idealized simulations of Cedar watershed runoff described in text. (a) Results from simulations where constant lapse rates of 4.0, 5.0, and 6.5 °C km⁻¹ are assumed (with solid, dashed, and dash-dotted lines respectively). (b) Results from simulations with seasonally varying PRISM lapse rates from the windward and lee domains (with solid and dash-dotted lines), as well as a constant 5.0 °C km⁻¹ (dashed). (c) Results from simulations of a 2°C climate warming (solid lines) with constant lapse rates of 5.0 and 6.5 °C km⁻¹. In all panels the runoff has been normalized by dividing by the basin area.

spring. This example illustrates not only the importance of correctly representing the mean lapse rate but also of correctly representing seasonal and regional variations.

[44] To investigate the consequences of lapse rate characterization for climate change projections we have also simulated the response of the Cedar basin to 2°C of climate warming at Cedar Lake COOP station with 5 or 6.5° C km⁻¹ lapse rates (Figure 9c). First, note that the effects of warming (Figure 9c) are of comparable magnitude to the effects of differing lapse rate assumptions (Figures 9a–9b) when considering wintertime peak flow or the timing of

melt season flow. Depending on the assumed lapse rate the effects of climate warming on the hydrograph differ. For instance, higher lapse rates result in smaller increases in Dec–Jan flow under warming, since they keep the upper reaches of the basin colder and accordingly less precipitation is converted from snow to rain under warming. The assumed lapse rate also strongly effects the impacts of warming at the end of the snowmelt season in July, with large lapse rates resulting in much more marked decreases in July flow under warming. These results reflect the specific hypsometry of the Cedar basin, its precipitation and temperature climatology, and the elevation of the station used to characterize the basin's climate. Thus, for other basins the impacts of assumed lapse rate will vary, but the impact will likely remain substantial if much of the snowpack resides at near-freezing temperatures.

5. Discussion and Conclusions

[45] We have characterized in detail the lapse rates for the Washington Cascades, and how they vary diurnally, seasonally, interannually, and geographically. The data sets we present give a characterization of the surface (and free air) lapse rates over regions ranging in scale from the Cascade Mountain range to a slope on Mount Rainier. The agreement between our varied data sets indicates that the results are largely robust on the regional scales considered. Still, our findings may not be particularly representative of the lapse rates in an individual mountain location. For instance, we showed in Figure 7 that inner-annual variability from a station pair on Mount Rainier is much different than that found in the upstream sounding. In light of such local effects, the regional-scale results presented here should be used only with caution when studying features on more local scales. Regional lapse rate estimates in Figures 3 and 4 may be adequate for studies of topics such as regional hydrology. However, these values may not be adequate for studies of topics such as local ecology and runoff from small basins, where site-specific controls on temperature necessitate local observations. The influence of local factors on lapse rates – particularly lapse rates derived from just two stations – also means that good regional estimates of lapse rates require extensive and multifaceted data sets.

[46] A particularly important finding is that the expedient assumption of a uniform and constant surface lapse rate of 6.5°C km⁻¹ is a poor one. While the difference between a mean lapse rate of 5.0°C km⁻¹ and 6.5°C km⁻¹ may seem trivial, we have shown that it can have pronounced consequences for mountain hydrology (Figure 9a). Also of importance are regional variations in lapse rates and their seasonality. Variations such as those occurring across the Cascades (Figure 6) are likely common for mountain ranges that separate maritime and continental climates, and also have major hydrological implications (Figure 9b).

[47] General lessons of this study are likely applicable to mountainous areas around the globe. Recent studies over other mountain ranges have also shown that 6.5°C km⁻¹ is not representative even of mean surface conditions, and that seasonal cycles in lapse rates have similar or greater amplitudes to those found in the Cascades, but the phasing of the seasonality varies [*Bolstad et al.*, 1998; *Rolland*, 2003; *Tang and Fang*, 2006; *Blandford et al.*, 2008; *Gardner et al.*,

2009]. Additionally, diurnal variations of surface lapse rates appear to be a fairly robust feature of mountain climates with several studies showing steeper lapse rates in daily maximum than daily minimum temperatures [e.g., *Bolstad et al.*, 1998; *Rolland*, 2003; *Blandford et al.*, 2008], although the magnitude of the diurnal variations differs between regions. Furthermore, the pronounced cross-mountain variations in lapse rates found in the Cascades are also apparent elsewhere [*Rolland*, 2003; *Tang and Fang*, 2006].

[48] The importance of the lapse rate for various applications combined with observations of strong lapse rate variability show it is vital that the gridding of climate data use lapse rates as consistent as possible with the observations. In estimating lapse rates from observations attention should be paid to the number and position of stations used: sites in deep valleys, mountain passes, and above glaciers each have distinctive characteristics that strongly affect the local temperature in ways that may not be representative of the larger terrain. When possible, the seasonal cycle of lapse rates, differences between free air and surface lapse rates, and regional differences in lapse rates should be considered.

[49] The PRISM analysis methodology appears to capture much of the spatial and seasonal variability apparent in other data sets. Thus, studies that use PRISM and similar products [e.g., *Elsner et al.*, 2009; *Loarie et al.*, 2009; *Weiss et al.*, 2009] likely suffer reduced temperature-related biases as compared to those that use cruder lapse rate assumptions for constructing temperature grids [e.g., *Hamlet et al.*, 2005; *Bales et al.*, 2006; *Bonfils et al.*, 2008]. However, since PRISM is built on observations, its performance is expected to degrade where there is sparse observational coverage. The success of MM5 at simulating lapse rate variability in this study shows that mesoscale numerical weather models are also valuable tools for mapping temperature, and may be of particular use in remote and complex terrain with minimal observations. However, further work must evaluate how well mesoscale models capture the details of the temperature distribution such as localized cool air pools and temperature inversions. Finally, at least for the Cascades, upwind soundings offer a fair representation of the seasonal cycle and annual mean of surface lapse rates on the windward slopes, providing yet another tool for temperature analysis when observations are sparse.

[50] The present study has largely stopped short of diagnosing the physical causes of lapse rate variability, however this is an important task. While the seasonality of lee side lapse rates appears to be clearly linked to behavior of cold air pools in the Columbia basin, many other aspects of the climatology remain unexplained. The primary processes controlling day-to-day and month-to-month variability, the seasonality over the windward slope, and differing values for "stormy" lapse rates are still unknown. Efforts to understand surface lapse rate variability in term of air mass characteristics (e.g., temperature and humidity), solar radiation, and synoptic flow patterns have reached differing conclusions as to the important controls [e.g., *Pepin et al.*, 1999; *Marshall et al.*, 2007; *Blandford et al.*, 2008]. A better understanding of the controls on mountain lapse rates in particular and mountain temperature patterns in general will be important for further improving climatological temperature analyzes and understanding present and future mountain climates. Achieving this will require synthesis of historical station data, experimental observational networks, sophisticated atmospheric models, and theory to recognize the dominant temperature patterns and their physical causes.

References

Anderson, E. A. (1976), A point energy and mass balance model of a snow cover, *NOAA Tech. Rep. 19*, U.S. Dept. of Comm., Silver Spring, Md.

Arnold, N. S., W. G. Rees, A. J. Hodson, and J. Kohler (2006), Topographic controls on the surface energy balance of a high Arctic valley glacier, *J. Geophys. Res.*, 111, F02011, doi:10.1029/2005JF000426.

Bales, R. C., N. P. Molotch, T. H. Painter, M. D. Dettinger, R. Rice, and J. Dozier (2006), Mountain hydrology of the western United States, *Water Resour. Res.*, 42, W08432, doi:10.1029/2005WR004387.

Bell, G. D., and L. F. Bosart (1988), Appalachian cold-air damming, *Monthly Weather Rev.*, 116(1), 137–161.

Blandford, T., K. Humes, B. Harshburger, B. Moore, V. Walden, and H. Ye (2008), Seasonal and synoptic variations in near-surface air temperature lapse rates in a mountainous basin, *J. Appl. Meteorol. Climatol.*, 47(1), 249–261, doi:10.1175/2007JAMC1565.1.

Bolstad, P. V., L. Swift, F. Collins, and J. Regniere (1998), Measured and predicted air temperatures at basin to regional scales in the southern Appalachian mountains, *Agric. For. Meteorol.*, 91(3–4), 161–176.

Bonfils, C., et al. (2008), Detection and attribution of temperature changes in the mountainous western United States, *J. Clim.*, 21(23), 6404–6424, doi:10.1175/2008JCLI2397.1.

Casola, J., L. Cuo, B. Livneh, D. Lettenmaier, M. Stoelinga, P. Mote, and J. Wallace (2009), Assessing the impacts of global warming on snowpack in the Washington Cascades, *J. Clim.*, 22(10), 2758–2772, doi:10.1175/2008JCLI2612.1.

Daly, C., W. P. Gibson, G. H. Taylor, G. L. Johnson, and P. Pasteris (2002), A knowledge-based approach to the statistical mapping of climate, *Clim. Res.*, 22(2), 99–113.

Daly, C., M. Halbleib, J. Smith, W. Gibson, M. Doggett, G. Taylor, J. Curtis, and P. Pasteris (2008), Physiographically sensitive mapping of climatological temperature and precipitation across the conterminous United States, *Int. J. Climatol.*, 28(15), 2031–2064, doi:10.1002/joc.1688.

Dodson, R., and D. Marks (1997), Daily air temperature interpolated at high spatial resolution over a large mountainous region, *Clim. Res.*, 8(1), 1–20.

Dooge, J. (1976), Linear theory of hydrologic systems, *Tech. Bull. 1468*, Agric. Res. Serv., U.S. Dept. of Agric., Alexandria, Va.

Elsner, M., L. Cuo, N. Voisin, J. Deems, A. Hamlet, J. Vano, K. Mickelson, S. Lee, and D. Lettenmaier (2009), Implications of 21st century climate change for the hydrology of Washington State, in *The Washington Climate Change Impacts Assesment: Evaluating Washington's Future in a Changing Climate*, Univ. of Wash., Seattle, Wash.

Gardner, A. S., M. J. Sharp, R. M. Koerner, C. Labine, S. Boon, S. J. Marshall, D. O. Burgess, and D. Lewis (2009), Near-surface temperature lapse rates over Arctic glaciers and their implications for temperature downscaling, *J. Clim.*, 22(16), 4281–4298, doi:10.1175/2009JCLI2845.1.

Grell, G. A., J. Dudhia, and D. R. Stauffer (1995), A description of the fifth-generation Penn State/NCAR mesoscale model (MM5), *NCAR Tech. Note NCAR/TN-398 1 STR*, Natl. Cent. for Atmos. Res., Boulder, Colo.

Hamlet, A. F., and D. P. Lettenmaier (2005), Production of temporally consistent gridded precipitation and temperature fields for the continental United States, *J. Hydrometeorol.*, 6(3), 330–336.

Hamlet, A. F., P. W. Mote, M. P. Clark, and D. P. Lettenmaier (2005), Effects of temperature and precipitation variability on snowpack trends in the western United States, *J. Clim.*, 18(21), 4545–4561.

Loarie, S. R., P. B. Duffy, H. Hamilton, G. P. Asner, C. B. Field, and D. D. Ackerly (2009), The velocity of climate change, *Nature*, *462*(7276), 1052–1055, doi:10.1038/nature08649.

Lundquist, J. D., and D. R. Cayan (2007), Surface temperature patterns in complex terrain: Daily variations and long-term change in the central Sierra Nevada, California, *J. Geophys. Res.*, *112*, D11124, doi:10.1029/2006JD007561.

Lundquist, J., and B. Huggett (2008), Evergreen trees as inexpensive radiation shields for temperature sensors, *Water Resour. Res.*, *44*, W00D04, doi:10.1029/2008WR006979.

Lundquist, J., P. Neiman, B. Martner, A. White, D. Gottas, and F. Ralph (2008), Rain versus snow in the Sierra Nevada, California: Comparing Doppler profiling radar and surface observations of melting level, *J. Hydrometeorol.*, *9*(2), 194–211, doi:10.1175/2007JHM853.1.

Marshall, S. J., M. J. Sharp, D. O. Burgess, and F. S. Anslow (2007), Near-surface-temperature lapse rates on the Prince of Wales Icefield, Ellesmere Island, Canada: Implications for regional downscaling of temperature, *Int. J. Climatol.*, *27*(3), 385–398, doi:10.1002/joc.1396.

Mass, C. F., et al. (2003), Regional environmental prediction over the Pacific Northwest, *Bull. Am. Meteorol. Soc.*, *84*(10), 1353–1366.

Maurer, E. P., A. W. Wood, J. C. Adam, D. P. Lettenmaier, and B. Nijssen (2002), A long-term hydrologically based dataset of land surface fluxes and states for the conterminous United States, *J. Clim.*, *15*(22), 3237–3251.

Minder, J., D. Durran, G. Roe, and A. Anders (2008), The climatology of small-scale orographic precipitation over the Olympic Mountains: Patterns and processes, *Q. J. R. Meteorol. Soc.*, *134*(633), 817–839, doi:10.1002/qj.258.

Mote, P. W., A. F. Hamlet, M. P. Clark, and D. P. Lettenmaier (2005), Declining mountain snowpack in western North America, *Bull. Am. Meteorol. Soc.*, *86*(1), 39–49.

Otto-Bliesner, B. L., S. J. Marsha, J. T. Overpeck, G. H. Miller, and A. X. Hu (2006), Simulating Arctic climate warmth and icefield retreat in the last interglaciation, *Science*, *311*(5768), 1751–1753, doi:10.1126/science.1120808.

Pepin, N. C., and D. J. Seidel (2005), A global comparison of surface and free-air temperatures at high elevations, *J. Geophys. Res.*, *110*, D03104, doi:10.1029/2004JD005047.

Pepin, N., D. Benham, and K. Taylor (1999), Modeling lapse rates in the maritime uplands of northern England: Implications for climate change, *Arct. Antarct. Alpine Res.*, *31*(2), 151–164.

Prentice, I. C., W. Cramer, S. P. Harrison, R. Leemans, R. A. Monserud, and A. M. Solomon (1992), A global biome model based on plant physiology and dominance, soil properties and climate, *J. Biogeogr.*, *19*(2), 117–134.

Rasmussen, L. A. (2009), South Cascade Glacier mass balance, 1935–2006, *Ann. Glaciol.*, *50*, 215–220.

Roe, G. H., and M. A. O'Neal (2010), The response of glaciers to intrinsic climate variability: Observations and models of late Holocene variations, *J. Glaciol.*, *55*(193), 839–854.

Rolland, C. (2003), Spatial and seasonal variations of air temperature lapse rates in Alpine regions, *J. Clim.*, *16*(7), 1032–1046.

Rowley, D. B., and C. N. Garzione (2007), Stable isotope-based paleoaltimetry, *Ann. Rev. Earth Planet. Sci.*, *35*, 463–508, doi:10.1146/annurev.earth.35.031306.140155.

Shamir, E., and K. P. Georgakakos (2006), Distributed snow accumulation and ablation modeling in the American River basin, *Adv. Water Resour.*, *29*(4), 558–570, doi:10.1016/j.advwatres.2005.06.010.

Smith, R. B., I. Barstad, and L. Bonneau (2005), Orographic precipitation and Oregon's climate transition, *J. Atmos. Sci.*, *62*(1), 177–191.

Snover, A. K., A. F. Hamlet, and D. P. Lettenmaier (2003), Climate-change scenarios for water planning studies: Pilot applications in the Pacific Northwest, *Bull. Am. Meteorol. Soc.*, *84*(11), 1513–1518.

Steenburgh, W. J., C. F. Mass, and S. A. Ferguson (1997), The influence of terrain-induced circulations on wintertime temperature and snow level in the Washington Cascades, *Weather Forecast.*, *12*(2), 208–227.

Stewart, I. T., D. R. Cayan, and M. D. Dettinger (2005), Changes toward earlier streamflow timing across western North America, *J. Clim.*, *18*(8), 1136–1155.

Tang, Z. Y., and J. Y. Fang (2006), Temperature variation along the northern and southern slopes of Mt. Taibai, China, *Agric. For. Meteorol.*, *139*(3–4), 200–207, doi:10.1016/j.agrformet.2006.07.001.

Wallace, J., and P. Hobbs (2006), *Atmospheric Science: An Introductory Survey*, 483 pp., Academic Press, Burlington, Mass.

Weiss, J., C. L. Castro, and J. Overpeck (2009), Distinguishing pronounced droughts in the southwestern United States: Seasonality and effects of warmer temperatures, *J. Clim.*, *22*(22), 5918–5932, doi:10.1175/2009JCLI2905.1.

White, A. B., D. J. Gottas, E. T. Strem, F. M. Ralph, and P. J. Neiman (2002), An automated brightband height detection algorithm for use with Doppler radar spectral moments, *J. Atmos. Oceanic Technol.*, *19*(5), 687–697.

Whiteman, C. D., S. Zhong, W. J. Shaw, J. M. Hubbe, X. Bian, and J. Mittelstadt (2001), Cold pools in the Columbia basin, *Weather Forecast.*, *16*(4), 432–447.

J. D. Lundquist, Department of Civil and Environmental Engineering, University of Washington, Box 352700, Seattle, WA 98195-2700, USA.

J. R. Minder, Department of Atmospheric Sciences, University of Washington, Box 351640, Seattle, WA 98195-1640, USA. (juminder@atmos.washington.edu)

P. W. Mote, Oregon Climate Change Research Institute, College of Oceanic and Atmospheric Sciences, Oregon State University, Strand Hall 326, Corvallis, OR 97331, USA.